Colloids and Surfaces A: Physicochem. Eng. Aspects 441 (2014) 504–509

Contents lists available at ScienceDirect

Colloids and Surfaces A: Physicochemical and Engineering Aspects

journal homepage: www.elsevier.com/locate/colsurfa

Dynamic adsorption process of phthalate at goethite/aqueous interface: An ATR-FTIR study

Yanli Yang, Jingjing Du, Chuanyong Jing*

State Key Laboratory of Environmental Chemistry and Ecotoxicology, Research Center for Eco-Environmental Sciences, Chinese Academy of Sciences, Beijing 100085, China

HIGHLIGHTS

- Phthalate adsorption at the goethite/aqueous interface was studied using ATR-FTIR.
- Phthalate form one outer-sphere and two bidentate inner-sphere surface complexes.
- Outer-sphere complex is suppressed with increasing ionic strength.
- Adsorption follow pseudo-second-order kinetics and reach equilibrium within 60 min.

GRAPHICAL ABSTRACT

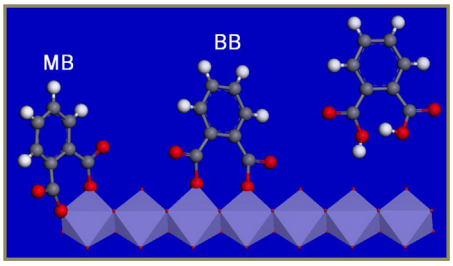

ARTICLE INFO

Article history:
Received 22 July 2013
Received in revised form
24 September 2013
Accepted 3 October 2013
Available online 12 October 2013

Keywords:
Phthalate
Goethite
ATR-FTIR spectroscopy
Surface complexation
Dynamic adsorption process

ABSTRACT

Insights into the molecular-level behaviors of phthalate at the goethite/aqueous interface can further our understanding of the fate and transport of natural organic matter analogs in the environment. The motivation of this work is to explore the interfacial configuration and dynamic adsorption process of phthalate on goethite at the molecular scale. The flow-cell ATR-FTIR measurement, curve-fitting analysis, and pseudo-second-order kinetic simulation were used to investigate the adsorption mechanisms. The results showed that phthalate formed one electrostatic outer-sphere complex and two inner-sphere configurations in mononuclear bidentate and binuclear bidentate structures. The contribution of outer-sphere complex to the overall phthalate adsorption was suppressed with increasing ionic strength and decreasing pH values. The ratio of adsorption capacity between these two inner-sphere configurations was slightly affected under different experimental conditions. Furthermore, the dynamic adsorption process of these three interfacial configurations followed the pseudo-second-order kinetics model, and reached equilibrium rapidly within 60 min.

1. Introduction

Phthalate is one of the ubiquitous low-molecular-weight carboxylic acid in the environment [1,2]. This carboxyl compound can readily adsorb onto minerals, thus altering its migration and susceptibility to transform in aquifers and soils. In addition, phthalate is deemed as an analog for natural organic matter (NOM) to investigate the mineral–NOM interactions, due to its high solubility in water, simple structure, as well as its similarity in functional groups to NOM [3–6]. Therefore, knowledge on the molecular-level mechanisms of phthalate adsorption is critical in understanding the interactions of NOM on minerals.

Extensive research has been conducted about phthalate adsorption on metal oxides using Fourier-transform infrared (FTIR) spectroscopy, but no consistent conclusion is obtained in its interfacial structure on the molecular level. For example, Tejedor-Tejedor [7] indicated that phthalate adsorbed on goethite in the form of mononuclear monodentate (M–M) and binuclear bidentate (B–B) structures involving only one carboxylate group bound to the surface iron. The B–B configuration was also observed by Dobson and McQuillan [8] for phthalate adsorption on TiO_2, ZrO_2, Al_2O_3, and Ta_2O_5. However, Persson et al. [9,10] proposed phthalate

* Corresponding author. Tel.: +86 10 62849523; fax: +86 10 62849523.
E-mail address: cyjing@rcees.ac.cn (C. Jing).

0927-7757/$ – see front matter © 2013 Elsevier B.V. All rights reserved.
http://dx.doi.org/10.1016/j.colsurfa.2013.10.021

adsorption on boehmite, aged γ-Al_2O_3, and goethite in outer-sphere and mononuclear bidentate (M–B) structures. Furthermore, Hwang [1] found that phthalate formed three surface complexes on hematite, namely a fully deprotonated outer-sphere complex and two inner-sphere complexes with respect to a M–B and a B–B complex involving both carboxylate groups. The discrepancy in the proposed interfacial configuration motivated our further investigation at the molecular-scale understanding of phthalate adsorption. Here, goethite was chosen as the model adsorbent, due to its ubiquity in terrestrial soils and sediment [11,12]. Moreover, the existing literature on goethite provides valuable references for comparison [7,10].

In this study, we investigated the adsorption mechanisms of phthalate at goethite/aqueous interface as a function of pH and ionic strength via in situ flow-cell measurements of attenuated total reflectance (ATR) FTIR spectroscopy. In addition to the determination of interfacial configurations, our current work focused on the dynamic process of phthalate adsorption on the basis of curve-fitting analysis and kinetic model simulation. These results could further our understanding of the fundamental interactions between NOM and iron oxide surfaces.

2. Experimental

2.1. Materials

High-purity phthalic acid was purchased from Sigma–Aldrich. All chemicals were analytical grade or higher and were used as received. The samples were prepared in Milli-Q water (18.2 MΩ), which was boiled for 60 min and cooled with N_2 purging to remove CO_2. Goethite was synthetized and characterized as shown in our previous reports [13,14]. The goethite had a N_2-BET surface area of 84.7 m^2/g and a point of zero charge (PZC) of 8.9.

2.2. ATR-FTIR spectroscopy study

The ATR-FTIR spectra were recorded with a Nicolet 6700 spectrometer equipped with a liquid-nitrogen cooled MCT detector. The ATR crystal, a 45° ZnSe or Ge crystal, was mounted in a flow cell (PIKE Technologies, USA). The pH range for ZnSe crystal was within 5–9, and the ZnSe crystal could be etched below pH 5. Then, Ge crystal was used when pH < 5. All spectra were averaged with 256 scans at 4 cm^{-1} resolution. Data collection and analysis were carried out with OMNIC software (Thermo Fisher Scientific Inc., USA). The numbers and positions of the frequency were justified using the second derivative. The curve-fitting analysis of the overlap peak within the wavenumber range 1470–1330 cm^{-1} was conducted using the Gaussian line shape [15,16].

The spectra of aqueous phthalate in 0.1 M NaCl solutions were obtained by subtracting the spectrum of background electrolyte solutions from the sample spectrum. The interfacial spectra of phthalate were measured with goethite film on the ZnSe crystal in the same way as our previous report [13,14]. Briefly, 400 μL of goethite suspensions (1 g/L) was spread on the crystal surface and dried in an oven at 50 °C for 1 h. Prior to use, the crystal was gently rinsed with Milli-Q water to remove loosely deposited goethite particles. Concentration of phthalic acid was fixed at 1 mM in 0.01, 0.1, and 1 M NaCl solution. The background electrolyte was passed through the flow cell at the rate of 0.4 mL/min, and the background spectrum was collected until the equilibrium was established. The solution was then changed to the sample with the same pH value and NaCl concentration as that in the background. The adsorbed spectra were recorded as a function of time for 150 min.

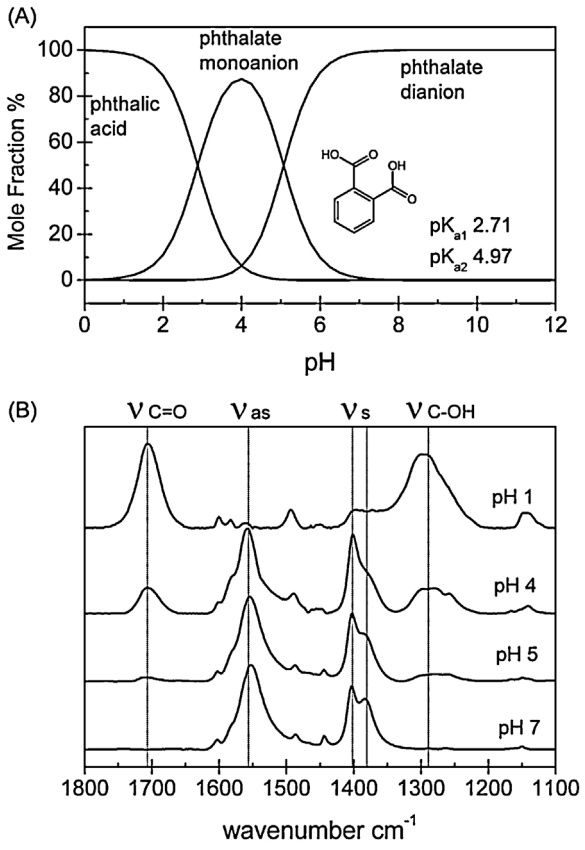

Fig. 1. (A) Distribution of phthalic acid, phthalate monoanion and dianion in solution as a function of pH at the ionic strength of 0.1 M. (B) FTIR spectra of 10 mM dissolved phthalic acid at pH 1, 4, 5, and 7 in 0.1 M NaCl solution. Spectra were normalized to the peak with the strongest intensity.

3. Results and discussion

3.1. ATR-FTIR spectroscopy of dissolved phthalate

Phthalic acid has two carboxylic groups with pK_{a1} = 2.71 and pK_{a2} = 4.97 at the ionic strength of 0.1 M, and thus exists as three aqueous species in the pH range 0–12 (Fig. 1A). The spectra of soluble phthalate at pH 1, 4, and 7 in Fig. 1B represent the phthalic acid, monoanionic phthalate, and dianionic phthalate species, respectively. The observed frequencies and peak assignments of dissolved phthalate are list in Table 1.

As for phthalate dianion, the bands at 1485 and 1443 cm^{-1} were associated with benzene ring vibrations [1,7,17–19]. The two peaks at 1383 and 1402 cm^{-1} were clearly resolved in the characteristic symmetric ν_{COO^-} region [1,9,19,20]. Similarly, the second derivative of the strong peak in the asymmetric ν_{COO^-} region revealed two components at 1554 and 1564 cm^{-1}, though it was seemed as a broad band at around 1552 cm^{-1} [9]. The appearance of asymmetric

Table 1
Peak positions and assignments for dissolved phthalate.

pH 1	pH 4	pH 7	Assignment
1709	1710		$\nu_{(C=O)}$
1565	1562	1564	$\nu_{as(COO)}$
1556	1556	1554	$\nu_{as(COO)}$
1494	1489	1485	$\nu_{CC(ring)}$
1448	1445	1443	$\nu_{CC(ring)}$
1402	1402	1402	$\nu_{s(COO)}$
1386	1384	1383	$\nu_{s(COO)}$
1290	1290		$\nu_{(C-OH)}$

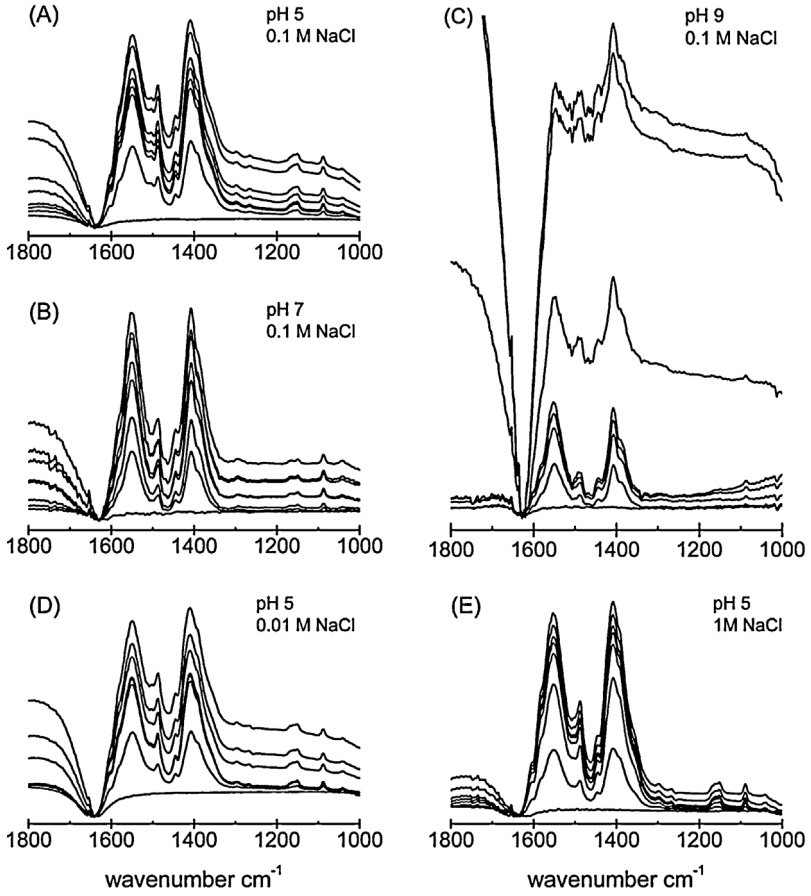

Fig. 2. The effect of pH and ionic strength on the dynamic spectra of adsorbed phthalate within 150 min.

and symmetric vibration modes could be attributed to the two equivalent COO^- groups which can move in cooperation or in opposition. The protonation of COO^- could increase asymmetry in the molecular structure, resulting in one single bond and one double bond. Consequently, the formation of one COOH group in phthalate monoanion resulted in the intensity increase at 1710 cm^{-1} associated with C=O stretch and a group of bands at ~1290 cm^{-1} with C—OH stretching vibration [1,18]. When fully protonated, the intensity of COOH vibrations further increased in accompany with a dramatic decrease in the intensity of COO^- vibrations. Consequently, the bands at ~1710 and 1290 cm^{-1} could be considered as sensitive indicators for the protonation of phthalate [21]. Furthermore, the benzene ring vibrations shifted upwards to 1494 and 1448 cm^{-1} upon full protonation of two COO^- groups.

3.2. Spectra of adsorbed phthalate at interface

In this study, we considered the effect of pH and ionic strength on the adsorption mechanisms of phthalate at goethite/aqueous interface (Fig. 2). Notably, the interfacial spectra from pH 9 in 0.1 M NaCl was in poor quality, due to the low adsorption capacity in basic conditions as well as the strong interference from vibrations associated with water. The limited adsorption capacity at high pH was also supported by the results of batch experiments in previous reports [1,4,18,22,23].

As shown in Fig. 2, the surface complex remained unchanged during adsorption at a certain pH or ionic strength, as evidenced by the same peak positions resolved by the second derivative in the dynamic spectra. Furthermore, the interfacial spectra in all investigated conditions exhibited similar frequencies, indicating the same interfacial configurations under different pH and ionic strength.

The interfacial spectra under investigated conditions exhibited two strong and heavily overlapped bands within the range of 1650–1300 cm^{-1}, which were roughly similar to that of phthalate dianion. Furthermore, contributions from the COOH vibrations of the protonated phthalate, i.e. $\nu_{C=O}$ at ~1710 cm^{-1} and ν_{C-OH} at ~1290 cm^{-1} were not evident, suggesting that the surface phthalate was in the dianionic form [1]. Notably, the spectra of dissolved phthalate at pH 5 represented spectroscopic feathers of monoanionic and dianionic phthalate species with relative content of 60% and 40%, respectively (Fig. 1B). Then, the absence of COOH vibrations of adsorbed spectra indicated that the existence of inner-sphere adsorption [1]. Thus, the number and type of specific surface complexes deserve our further study.

3.3. Determination of the interfacial configurations

In this investigation, we focus on the analysis of symmetric COO^- stretching region within 1460–1300 cm^{-1}, because the interfacial spectra were strongly affected by the interference from vibrations associated with water. The intense of H—O—H bending vibrations are strongest near 1640 cm^{-1} and extend into the asymmetric COO^- stretching region within 1600–1450 cm^{-1}, strongly affecting the accuracy of analysis (i.e. determination of the overlapped bands, baseline normalization, and curve-fitting procedure). In contrast, the vibrations associated with water bending do not extend below 1450 cm^{-1} and thus do not impact the symmetric COO^- stretch. Furthermore, the asymmetric and symmetric COO^- stretch vibrations appear in pairs, thus the surface complex could be determined from the number and positions of the symmetric COO^- stretch vibrations.

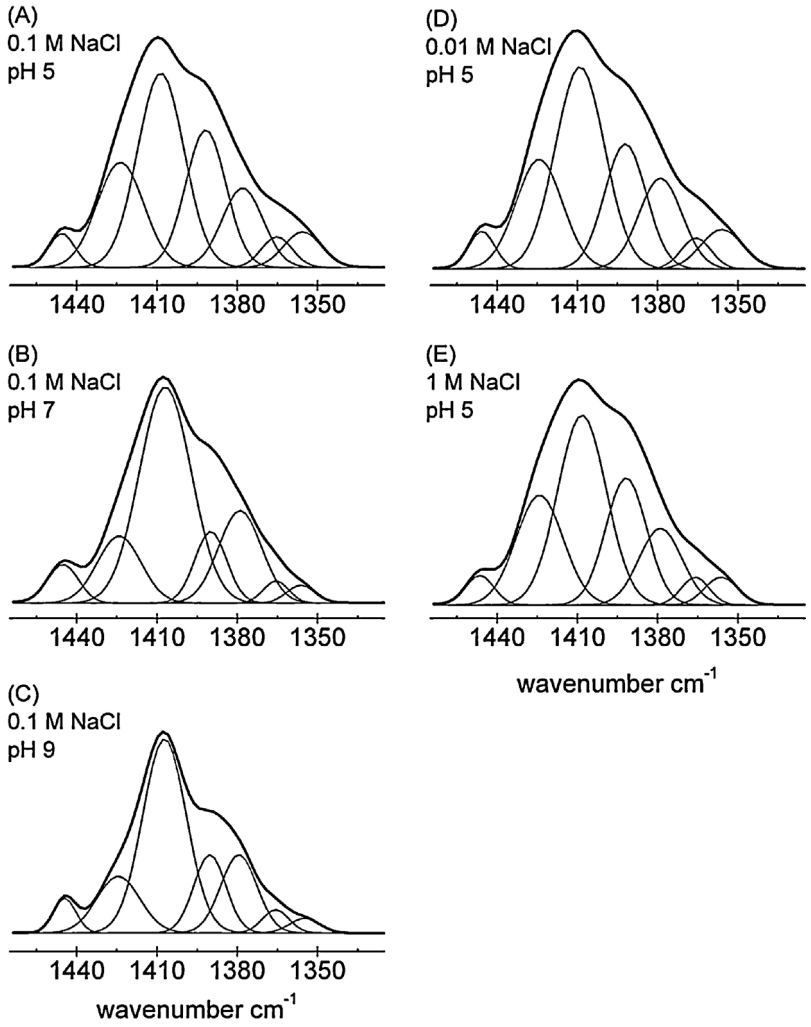

Fig. 3. Curve-fitting results of the overlapped peaks within 1450–1300 cm^{-1} from the time-dependent spectra collected at 150 min.

Based on the second derivative method, the overlapped peaks within symmetric COO^- stretching region were further analyzed by the curve fitting procedure in high quality (r^2 = 0.99). The results of the spectra collected at 150 min were shown in Fig. 3 for illustration. The band centered at ~1445 cm^{-1} was attributed to benzene ring vibrations [19]. As suggested by previous studies, the six bands at ~1423, 1407, 1391, 1378, 1365, and 1356 cm^{-1} should be all associated with symmetric $\nu_{S(COO^-)}$ modes [1,9,20]. As discussed above, the adsorbed phthalate was in the dianionic form, indicating two symmetric COO^- stretch vibrations in a certain surface complex. Consequently, six symmetric COO^- stretch vibrations in this study suggested the existence of at least three surface complexes. The determination of interfacial configurations and peaks belonging to each structure were list in Table 2.

Table 2
Peak positions and assignments for adsorbed phthalate in outer-sphere, mononuclear bidentate (M–B), and binuclear bidentate (B–B) structures.

Outer-sphere	M–B	B–B	Assignment
~1445			$\nu_{CC(ring)}$
		~1423	$\nu_{s(COO)}$
~1407			$\nu_{s(COO)}$
	~1391		$\nu_{s(COO)}$
~1378			$\nu_{s(COO)}$
		~1365	$\nu_{s(COO)}$
	~1356		$\nu_{s(COO)}$

In line with previous studies, we also resolved the coexistence of outer-sphere and inner-sphere adsorption mechanisms of phthalate on goethite [22]. The bands centered at ~1445, 1407 and 1378 cm^{-1} in the interfacial spectra were in close similarity to 1443, 1402 and 1383 cm^{-1} of the phthalate dianion, which could be attributed to the outer-sphere complex [1]. The non-specific adsorption interactions were also observed for phthalate on iron and aluminum (hydr)oxides [1,9,20,22].

The other four peaks at ~1423, 1391, 1365, and 1356 cm^{-1} shifted significantly from that of the symmetric $\nu_{S(COO^-)}$ vibrations of dissolved phthalate, corresponding to two inner-sphere complexes. These four bands were of similar peak positions with those of phthalate on hematite reported by Hwang et al. [1]. Compared with the frequencies of phthalate dianion, the symmetric COO^- stretch vibrations of M–B configuration shifted downwards to ~1391 and 1356 cm^{-1} [1]. In contrast, the two bands at ~1423 and 1365 cm^{-1} attributable to the B–B structure were shifted from ~1402 and 1383 cm^{-1} of the phthalate dianion, respectively [1]. Notably, the ~1365 cm^{-1} peak was not resolved by Hwang by means of spectral subtraction, probably because of the weak intensity and close peak position in comparison with those of ~1365 cm^{-1} (Fig. 3). Furthermore, the M–B and B–B type complexes coordinated to the surface iron via one oxygen atom from each COO^- group of the phthalate dianion, due to the absence of bands at ~1710 and 1290 cm^{-1} associated with protonated COOH vibrations.

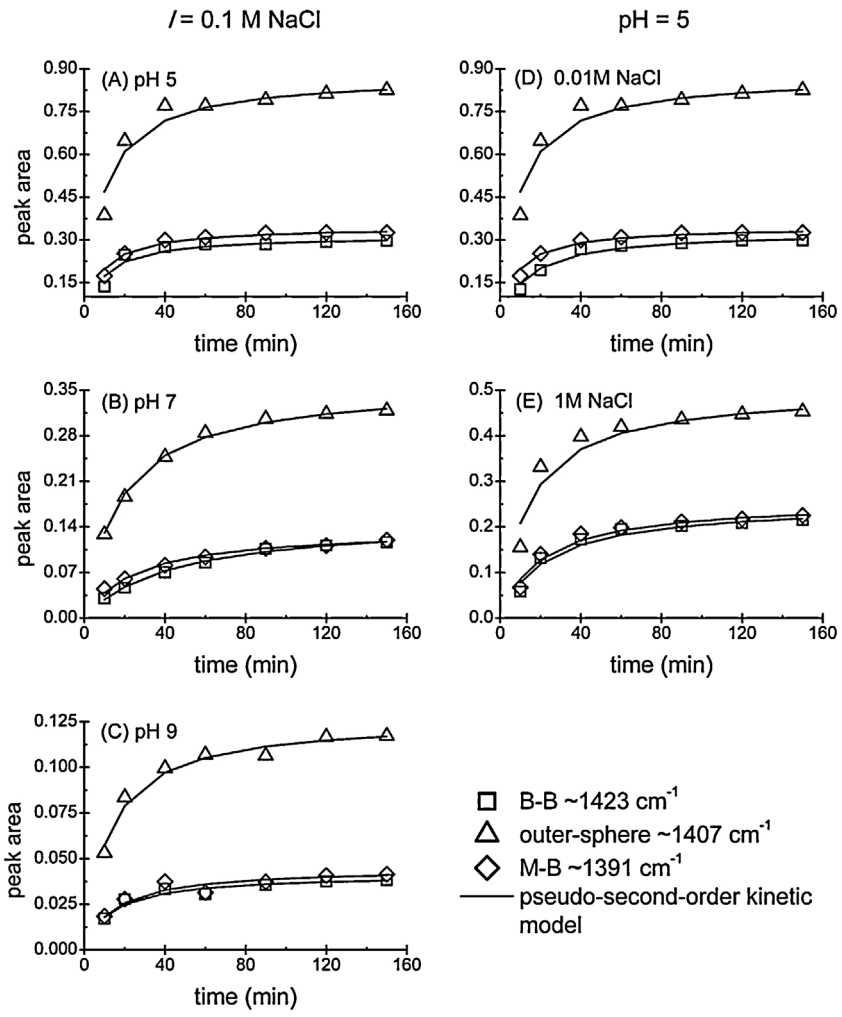

Fig. 4. Dynamic change in areas of the peak at ~1423, 1407, and 1391 cm^{-1} under different pH and ionic strength.

3.4. Dynamic adsorption process of phthalate on goethite

The dynamic adsorption process for each interfacial configuration could be illustrated by monitoring the changes of their corresponding peak areas along with time [13,15,16,24]. The peak areas within the 1460–1300 cm^{-1} range were obtained via curve-fitting procedure. The fitting parameters, i.e. individual peak position and height, as well as full width at half maximum, were chosen on the basis of minimized residual between the overall fit and experimental spectrum. As shown in Fig. 4, the peaks at ~1423, 1407, and 1391 cm^{-1} were selected for representing the B–B, outer-sphere, and M–B structures, respectively.

The three surface complexes exhibited similar adsorption behaviors in the dynamic process under all conditions. The adsorption capacity increased along with time and reached equilibrium rapidly within about 60 min. Furthermore, the dynamic process of phthalate adsorption followed the pseudo-second-order kinetic model [5,25,26]:

$$\frac{t}{q_t} = \frac{1}{kq_e^2} + \frac{1}{q_e}t$$

Here, q_t is the peak area of a certain configuration at time t; q_e is the equilibrium uptake; k is the equilibrium rate constant of pseudo-second-order kinetics. The values of q_e and k were calculated from the linear fitting parameters of t/q_t versus t. The constant parameters and correlation coefficients were summarized in Table 3.

3.5. The effect of pH and ionic strength on phthalate adsorption

The three surface complexes were of different adsorption capacity as a function of pH and ionic strength, due to the uneven enhancement in the shape of overlapped peaks within the range of 1650–1300 cm^{-1} [13,24]. The interfacial spectra were roughly similar to that of the phthalate dianion, suggesting that the outer-sphere adsorption was the dominant mechanisms on the molecular level. Furthermore, the strong dependence of macroscopic adsorption on pH and ionic strength also indicates the significant contribution of electrostatic interactions between phthalate and goethite surface.

As shown in Fig. 4, high pH suppressed the contribution of inner-sphere complex to the overall phthalate adsorption where the outer-sphere species are predominant, as evidenced by the ratio in peak areas of ~1423, 1407, and 1391 cm^{-1} obtained at 150 min in 0.1 M NaCl, i.e. 0.45:1:0.47 (pH 5), 0.37:1:0.38 (pH 7), and 0.33:1:0.35 (pH 9). The inhibition of high pH on inner-sphere adsorption was also observed for other pure carboxylates such as tricarballylate [27]. Furthermore, the relative content of outer-sphere complex to the overall adsorption was decreased along with increasing ionic strength, which was evidenced by the ratios of the peak area of 1423, 1407, and 1391 cm^{-1} obtained at 150 min, i.e. 0.36:1:0.39, 0.45:1:0.47, and 0.48:1:0.51 for pH 5 in 0.01, and 0.1, and 1 M NaCl solution, respectively. The decrease in the formation of outer-sphere complexes in high ionic strength could be attributed to the strong competition from chloride. However, no significant discrepancies were observed on the ratio of adsorption

Table 3
Constant parameters and correlation coefficients for the pseudo-second-order kinetic model.

	Peak position (cm^{-1})	0.01 M NaCl		0.1 M NaCl		1 M NaCl	
		r^2	k	r^2	k	r^2	k
	~1423	0.998	0.2398	0.9973	0.3894	0.9886	0.1784
pH 5	~1407	0.9982	0.1323	0.9982	0.1324	0.9937	0.1413
	~1391	0.9992	0.3846	0.9992	0.3846	0.9935	0.1938
	1423			0.9958	0.1539		
pH 7	1407			0.9994	0.1596		
	1390			0.9967	0.2911		
	1423			0.9944	1.828		
pH 9	1406			0.9977	0.6572		
	1390			0.9882	1.5155		

Note. r and k refer to the correlation coefficient and equilibrium rate constant, respectively.

capacity between M–B and B–B inner-sphere configurations under different pH and ionic strength conditions.

4. Conclusions

The dynamic adsorption process of phthalate at goethite/aqueous interface was investigated via ATR-FTIR flow-cell measurement under different pH and ionic strength. The interfacial spectra with 1 mM phthalate in 0.01 and 0.1 M NaCl resolved the coexistence of one outer-sphere and two inner-sphere surface complexes. The outer-sphere complex adsorbed on goethite via electrostatic interactions, and the inner-sphere complexes were in M–B and B–B structures with one oxygen atom from each COO^- group of the phthalate dianion coordinated to the surface iron. As for the dynamic process, the three surface complexes reached adsorption equilibrium rapidly within about 60 min, and could be well described by the pseudo-second-order kinetics model. The results provide insights into the molecular-level mechanisms of phthalate adsorption on goethite, facilitating description and prediction of the behaviors of NOM in the environmental.

Acknowledgement

We acknowledge the financial support of the National Natural Science Foundation of China (41023005, 41373123 and 21321004).

Appendix A. Supplementary data

Supplementary data associated with this article can be found, in the online version, at http://dx.doi.org/10.1016/j.colsurfa.2013.10.021.

References

[1] Y.S. Hwang, J. Liu, J.J. Lenhart, C.M. Hadad, Surface complexes of phthalic acid at the hematite/water interface, J. Colloid Interface Sci. 307 (2007) 124–134.
[2] B.W. Strobel, Influence of vegetation on low-molecular-weight carboxylic acids in soil solution—a review, Geoderma 99 (2001) 169–198.
[3] C.C. Trout, J.D. Kubicki, UV resonance Raman spectra and molecular orbital calculations of salicylic and phthalic acids complexed to Al^{3+} in solution and on mineral surfaces, J. Phys. Chem. A 108 (2004) 11580–11590.
[4] C.R. Evanko, D.A. Dzombak, Influence of structural features on sorption of NOM-analogue organic acids to goethite, Environ. Sci. Technol. 32 (1998) 2846–2855.
[5] X.H. Guan, G.H. Chen, C. Shang, Combining kinetic investigation with surface spectroscopic examination to study the role of aromatic carboxyl groups in NOM adsorption by aluminum hydroxide, J. Colloid Interface Sci. 301 (2006) 419–427.
[6] X.H. Guan, C. Shang, G.H. Chen, Competitive adsorption of organic matter with phosphate on aluminum hydroxide, J. Colloid Interface Sci. 296 (2006) 51–58.
[7] M.I. Tejedor-Tejedor, E.C. Yost, M.A. Anderson, Characterization of benzoic and phenolic complexes at the goethite/aqueous solution interface using cylindrical internal reflection Fourier transform infrared spectroscopy. 2. Bonding structures, Langmuir 8 (1992) 525–533.
[8] K.D. Dobson, A.J. McQuillan, In situ infrared spectroscopic analysis of the adsorption of aromatic carboxylic acids to TiO_2, ZrO_2, Al_2O_3, and Ta_2O_5 from aqueous solutions, Spectrochim. Acta A 56 (2000) 557–565.
[9] J. Nordin, P. Persson, E. Laiti, S. Sjöberg, Adsorption of o-phthalate at the water–boehmite (γ-AlOOH) interface: evidence for two coordination modes, Langmuir 13 (1997) 4085–4093.
[10] P. Persson, J. Nordin, J. Rosenqvist, L. Lövgren, L.O. Öhman, S. Sjöberg, Comparison of the adsorption of o-phthalate on boehmite (γ-AlOOH), aged γ-Al_2O_3, and goethite (α-FeOOH), J. Colloid Interface Sci. 206 (1998) 252–266.
[11] S. Kang, D. Amarasiriwardena, B. Xing, Effect of dehydration on dicarboxylic acid coordination at goethite/water interface, Colloids Surf. A 318 (2008) 275–284.
[12] A.J.A. Aquino, D. Tunega, G. Haberhauer, M.H. Gerzabek, H. Lischka, Acid–base properties of a goethite surface model: a theoretical view, Geochim. Cosmochim. Acta 72 (2008) 3587–3602.
[13] Y. Yang, W. Yan, C. Jing, Dynamic adsorption of catechol at the goethite/aqueous solution interface: a molecular-scale study, Langmuir 28 (2012) 14588–14597.
[14] Y. Yang, J. Duan, C. Jing, Molecular-scale study of salicylate adsorption and competition with catechol at goethite/aqueous solution interface, J. Phys. Chem. C 117 (2013) 10597–10606.
[15] S.J. Hug, In situ Fourier transform infrared measurements of sulfate adsorption on hematite in aqueous solutions, J. Colloid Interface Sci. 188 (1997) 415–422.
[16] J. Ha, T. Hyun Yoon, Y. Wang, C.B. Musgrave, J.G.E. Brown, Adsorption of organic matter at mineral/water interfaces: 7. ATR-FTIR and quantum chemical study of lactate interactions with hematite nanoparticles, Langmuir 24 (2008) 6683–6692.
[17] J.S. Loring, M. Karlsson, W.R. Fawcett, W.H. Casey, Infrared spectra of phthalic acid, the hydrogen phthalate ion, and the phthalate ion in aqueous solution, Spectrochim. Acta A 57 (2001) 1635–1642.
[18] M.R. Das, S. Mahiuddin, The influence of functionality on the adsorption of p-hydroxy benzoate and phthalate at the hematite–electrolyte interface, J. Colloid Interface Sci. 306 (2007) 205–215.
[19] S. Tunesi, M.A. Anderson, Surface effects in photochemistry: an in situ cylindrical internal reflection-Fourier transform infrared investigation of the effect of ring substituents on chemisorption onto titania ceramic membranes, Langmuir 8 (1992) 487–495.
[20] O. Klug, W. Forsling, A spectroscopic study of phthalate adsorption on γ-aluminum oxide, Langmuir 15 (1999) 6961–6968.
[21] P.M. Morris, R.A. Wogelius, Phthalic acid complexation and the dissolution of forsteritic glass studied via in situ FTIR and X-ray scattering, Geochim. Cosmochim. Acta 72 (2008) 1970–1985.
[22] J.F. Boily, P. Persson, S. Sjöberg, Benzenecarboxylate surface complexation at the goethite (α-FeOOH)/water interface: II. Linking IR spectroscopic observations to mechanistic surface complexation models for phthalate, trimellitate, and pyromellitate, Geochim. Cosmochim. Acta 64 (2000) 3453–3470.
[23] J.F. Boily, P. Persson, S. Sjöberg, Benzenecarboxylate surface complexation at the goethite (α-FeOOH)/water interface: III. The influence of particle surface area and the significance of modeling parameters, J. Colloid Interface Sci. 227 (2000) 132–140.
[24] K. Axe, M. Vejgården, P. Persson, An ATR-FTIR spectroscopic study of the competitive adsorption between oxalate and malonate at the water–goethite interface, J. Colloid Interface Sci. 294 (2006) 31–37.
[25] Y. Liu, New insights into pseudo-second-order kinetic equation for adsorption, Colloids Surf. A 320 (2008) 275–278.
[26] M. Yurdakoç, Y. Seki, S. Karahan, K. Yurdakoç, Kinetic and thermodynamic studies of boron removal by Siral 5, Siral 40, and Siral 80, J. Colloid Interface Sci. 286 (2005) 440–446.
[27] M. Lindegren, J.S. Loring, P. Persson, Molecular structures of citrate and tricarballylate adsorbed on α-FeOOH particles in aqueous suspensions, Langmuir 25 (2009) 10639–10647.